Catalysis Letters Vol. 109, Nos. 1–2, June 2006 (© 2006)
DOI: 10.1007/s10562-006-0050-x

PtRu colloid nanoparticles for CO oxidation in microfabricated reactors

Asbjørn Klerke,[a] Souheil Saadi,[b] Maja Bøg Toftegaard,[a] Anders Theilgaard Madsen,[a] Jane H. Nielsen,[b] Søren Jensen,[c] Ole Hansen,[b,c] Claus Hviid Christensen,[a] and Ulrich J. Quaade[b,*]

[a]*Danish National Research Foundation's Center for Sustainable and Green Chemistry (CSG), Department of Chemistry, Technical University of Denmark, 2800 Kgs Lyngby, Denmark*
[b]*Danish National Research Foundation's Center for Individual Nanoparticle Functionality (CINF), Department of Physics, Technical University of Denmark, 2800 Kgs Lyngby, Denmark*
[c]*MIC – Department of Micro and Nanotechnology, Technical University of Denmark, 2800 Kgs Lyngby, Denmark*

Received 15 December 2005; accepted 1 March 2006

The catalytic activity of PtRu colloid nanoparticles for CO oxidation is investigated in microfabricated reactors. The measured catalytic performance describes a volcano curve as a function of the Pt/Ru ratio. The apparent activation energies for the different alloy catalysts are between 21 and 117 kJ/mol, which agree well with literature. The size distribution of the colloid nanoparticles is determined from STM and TEM, from which an average size of the colloid nanoparticles of 2.2 ± 0.5 nm is determined.

KEY WORDS: CO oxidation; heterogeneous catalysis; nanoparticles; colloids; alloyed nanoparticles; platinum and ruthenium.

1. Introduction

Selective CO oxidation is an important reaction when hydrogen is produced by steam-reforming of hydrocarbons for use in proton exchange membrane fuel cells (PEMFC) since the common anodic catalyst in PEMFC is severely poisoned by CO even in minute quantities [1, 2]. This deactivation of the anodic catalyst can be avoided if CO is completely oxidized to CO_2 because the anode tolerance for CO_2 is much higher than it is for CO.

Several different catalysts have been proposed for the selective catalytic oxidation of CO, for example metal oxides [3, 4] and noble metals [5, 6] with a special emphasis on platinum and ruthenium [7–10]. This special interest in Pt and Ru has been substantiated through theoretical studies of CO desorption on platinum, ruthenium and an alloy of Pt and Ru [11–13]. The studies show that such an alloy has a significantly lower desorption energy for CO than both of the pure metals. This lower desorption energy gives the possibility of a higher catalytic activity, as CO covering the surface of the catalyst is most probably an important limiting factor for the activity.

Here, we report and discuss the use of PtRu alloys for the oxidation of CO in microfabricated reactors. It is found that an easy method for preparing alloys of PtRu is to synthesize colloid nanoparticles [14]. To form these colloids, Pt^{4+} and Ru^{3+} precursors are reduced to PtRu colloids in alkaline ethylene glycol solutions where ethylene glycol acts as a reducing agent and a colloid stabilizer at the same time. The size of the colloid PtRu nanoparticles is controlled by the concentration of sodium hydroxide present during reduction. The metal concentration is not important for the colloid nanoparticle size when the reaction mixture does not contain water [15].

Colloids can be stabilized in solutions in different ways. In this investigation, the stabilization is mainly thought to be electrostatic as illustrated in figure 1.

The charged colloid nanoparticles are stabilized by the positive dipolar moment of the colloid surface, which forms a shield of negatively charged ions in the stabilizing solvent which effectively prevents agglomeration due to electrostatic repulsion between neighboring colloid particles [16].

Colloid particles have previously been used in different catalytic reactions, but mostly for organic syntheses [17]. The use of colloids represents an elegant approach to prepare metal alloy catalysts featuring uniform nanoparticles with well-controlled size and composition [18, 19]. The process of making colloid particles is also simple and therefore practical in laboratory experiments.

The use of colloid particles in a microfabricated reactor is furthermore an advantage because the small reactor gives optimal conditions with possibilities for high space velocity in a well-defined laminar flow and for rapid temperature changes [20–22]. The experimental setup also provides fast response to changes in the reaction conditions.

There are two major advantages of using microfabricated reactors. First, the large surface to volume ratio

*To whom correspondence should be addressed.
E-mail: Quaade@fysik.dtu.dk

1011-372X/06/0600–0007/0

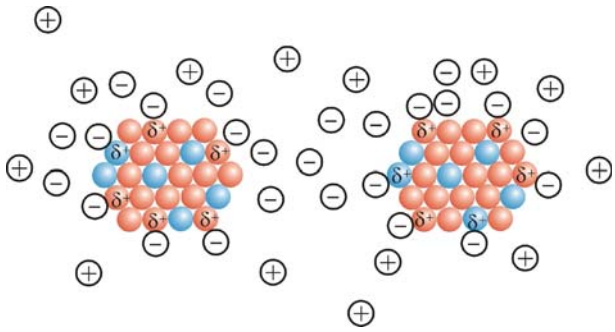

Figure 1. Schematic representation of electrostatic stabilization of PtRu colloid nanoparticles. The core consists of partially positively charged metal atoms and is stabilized by the negatively charged ions in the solvent.

enables quantitative detection of reaction products from less than a monolayer of non-porous catalyst deposited in the bottom on the reactor. Second, colloids deposited on a flat substrate like the reactor bottom are expected to be fairly mobile and suffer from agglomeration and sintering resulting in deactivation of the catalyst. This is not prevented in microreactors but with the fast response in microreactors, the characterization time can be short compared to the timescale of deactivation.

The size of the reactor is also of importance if it – in a future perspective – is used in connection with a transportable fuel cell system. A small size CO oxidizer is advantageous if hydrogen is generated from carbon containing sources such as methanol, ethanol or methane.

2. Experimental

2.1. Colloid particle preparation

The colloid particles of varying Pt/Ru ratios are prepared according to the method described by Bock *et al.* [14] using 0.065 M sodium hydroxide in ethylene glycol as the stabilizer and reducing agent. This gives the possibility of lowering the metal concentration without affecting the size of the colloid particles [15]. The combined concentration of Pt^{4+} and Ru^{3+} is 0.0082 M prepared from $PtCl_4$ and $RuCl_3$.

To form the colloid particles, the reaction mixture is heated to 160 °C for 3 h with reflux in a stirred oil bath. Then it is cooled and transferred to storage bottles. Prior to its use, the colloid solution is diluted 1:40. This is done to ensure that particle coverages of 10–20% are obtained in the microfabricated reactor when adding a controlled volume of colloid solution.

2.2. Scanning tunneling microscopy

The STM measurements are carried out using an EasyScan STM from Nanosurf AG. All measurements are performed at room temperature in atmospheric air. Substrates consisting of silicon covered by 2 μm gold deposited by e-beam deposition are used. The sample discs are prepared by gluing the gold-coated silicon substrate to a steel sample holder using conducting glue.

Initially, the gold surface is characterized with the STM before the colloid particles are deposited. Then 4 μL of the diluted colloid solution is placed on the gold surface for 2 min and cleaned off with ethanol. The sample is dried in air and placed in the STM for investigation of the size distribution of the colloid nano particles.

During the constant current mode measurements, the gap voltage is 0.40 V and the tunnel current is fixed at 1 nA. This setting gave the best results with our equipment.

2.3. Transition electron microscopy

The particle size distribution is also determined with transmission electron microscopy (TEM) and a dark-field TEM (DF-TEM) in a JEOL 3000 F electron microscope operated at 300 keV and a chamber pressure of 10^{-8} Pa. The images are recorded by a 4× 4 k CCD detector.

The colloid particle solution is diluted by adding two drops of the concentrated colloid solution into 100 mL of ethanol. The solution is ultrasonically suspended for 60 s. This is done to prevent heavy agglomeration of the particles. Several drops of the suspension are applied to an amorphous carbon film on a 200 Cu grid (Lacey). Estimated particle size distributions are obtained by accurately determining the sizes of 20–60 particles in representative TEM images selected for each sample.

2.4. Preparation of microfabricated reactors

The microfabricated reactors are produced on silicon substrates by deep reactive ion etching (DRIE), sealed using anodic bonding and interfaced according to earlier reports [22, 23]. The reaction chamber has dimensions of 15 mm × 1.5 mm × 0.3 mm.

The microfabricated reactors are cleaned with acetone before they are loaded with 2 μL of the 1:40 diluted colloidal solution and heated to 80 °C to evaporate the solvent. This corresponds to a calculated total number of deposited particles of 1.1×10^{12}, assuming that all particles are spherical with a radius of 1.1 nm. This gives an estimated coverage of the reactor bottom of 19% and a total of 2.4×10^{14} surface atoms. Figure 2 shows a photograph of a bonded microfabricated reactor with colloids (not visible) inside, prior to any reactivity measurements.

2.5. Experimental setup

The microfabricated reactor is mounted on an aluminum interface and the gas inlet and outlet are sealed with Viton o-rings to make gas tight seals. A silicon heating element is mounted on the back of the reactor

Figure 2. Microfabricated reactor after anodic bonding with colloids inside. The gas inlet and outlet are seen in the left side of the picture.

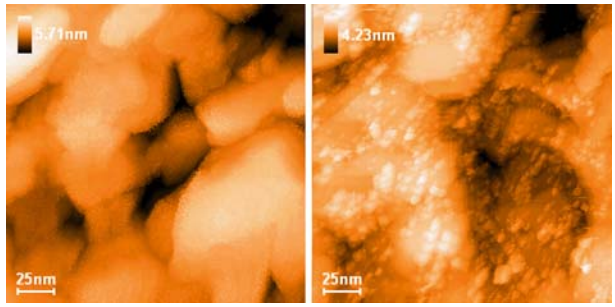

Figure 3. Left: STM image of a clean Au surface with large Au islands. Right: STM image of Au surface with PtRu colloid nanoparticles that are seen as small dots with a size of 2–5 nm. Some particles are agglomerated into slightly larger structures.

chamber. The temperature is measured using an infrared temperature sensor focused onto the reactor channel. The heating is controlled by a PID feed-back algorithm, and the temperature is sampled once a second with a precision of 0.1 °C.

The gas flow is controlled with a mass flow controller in the region from 0 to 1 mL/min with a precision of 0.02 mL/min. The reaction gas is premixed and contains 5% CO, 2.5% O_2, 2.5% Ar in He.

To measure the catalytic performance, a mass spectrometer (MS) is connected to the reactor outlet and Ar is used as an internal standard. During activity measurements, the ion currents for the mass/charge ratios (m/q) of 28 (CO and N_2), 32 (O_2), 40 (Ar) and 44 (CO_2) are recorded.

2.6. Measuring the catalytic activity

Measurements of the catalytic activity are carried out in two steps. First an activation cycle in which the reactor is heated in a gas flow of 1 mL/min of the reaction gas from an initial temperature of 225–310 °C at a constant rate of 10 K/min. Then, the temperature is kept constant for 30 min before cooling down to 225 °C at a rate of 10 K/min. The colloid particles deposited in the bottom of the reactor are expected to be fairly mobile causing agglomeration and sintering. The activation cycle ensures that the microfabricated reactor is in a steady state during the activity measurement since any deactivation due to agglomeration or sintering of the colloid nanoparticles occurred before the activity measurements. Furthermore, any organic remnants from the synthesis are oxidized.

Following the activation cycle, activity measurements are carried out with a gas flow of 0.5 mL/min and temperature ramps from 250 to 340 °C with a rate of 5 K/min. The temperature is kept constant at 340 °C for 5 min and then ramped back to 250 °C at the same rate.

3. Result and discussion

The deposited colloid particles were studied by TEM and STM to verify that the size distribution agrees with that reported in the original experiments [14] and that the particles are evenly distributed on the surface of the reactor. Figure 3 (left) shows a clean gold surface with steps and terraces. The surface appears to consist of smooth Au islands larger than 50 nm.

In figure 3(right), this is compared to the gold surface with deposited colloid nanoparticles. The colloid particles are easily seen as small dots.

The sizes of the colloid nanoparticles are generally found to vary between 2 and 5 nm but some large agglomerates are also observed. However, this might not be an accurate size determination since it could be influenced by broadening effects from ethylene glycol residues and from the tip. Furthermore, it is difficult to make precise determinations of the colloid size because the gold surface is not completely flat. To get an independent determination of the size distribution the colloid particles were also investigated using TEM. The TEM images of PtRu colloids show well-defined particles for all the investigated samples as shown in figure 4, although the crystal planes are not resolved. As for the STM measurements some agglomeration is observed, which is expected from the drying process. The measured size distributions determined by TEM are shown in figure 5. It is seen that all the compositions of colloids have particle sizes within the same size range and slightly smaller than the 3.5 ± 1.5 nm for 0.065 M NaOH expected from the data of Bock *et al.* [14]. This may be because our initial metal concentration is significantly lower and this influences the size of the colloids, even if this was not expected [14].

For investigating the activity as a function of the catalyst composition a selection of different colloid solutions is prepared. The compositions, and Pt and Ru concentrations can be seen in table 1. For each composition, microreactors are prepared with similar amounts of colloids and activity measurements are performed.

3.1. Catalytic activity

Data from an activation cycle of a reactor containing Pt 55%–Ru 45% colloids are shown in figure 6, where

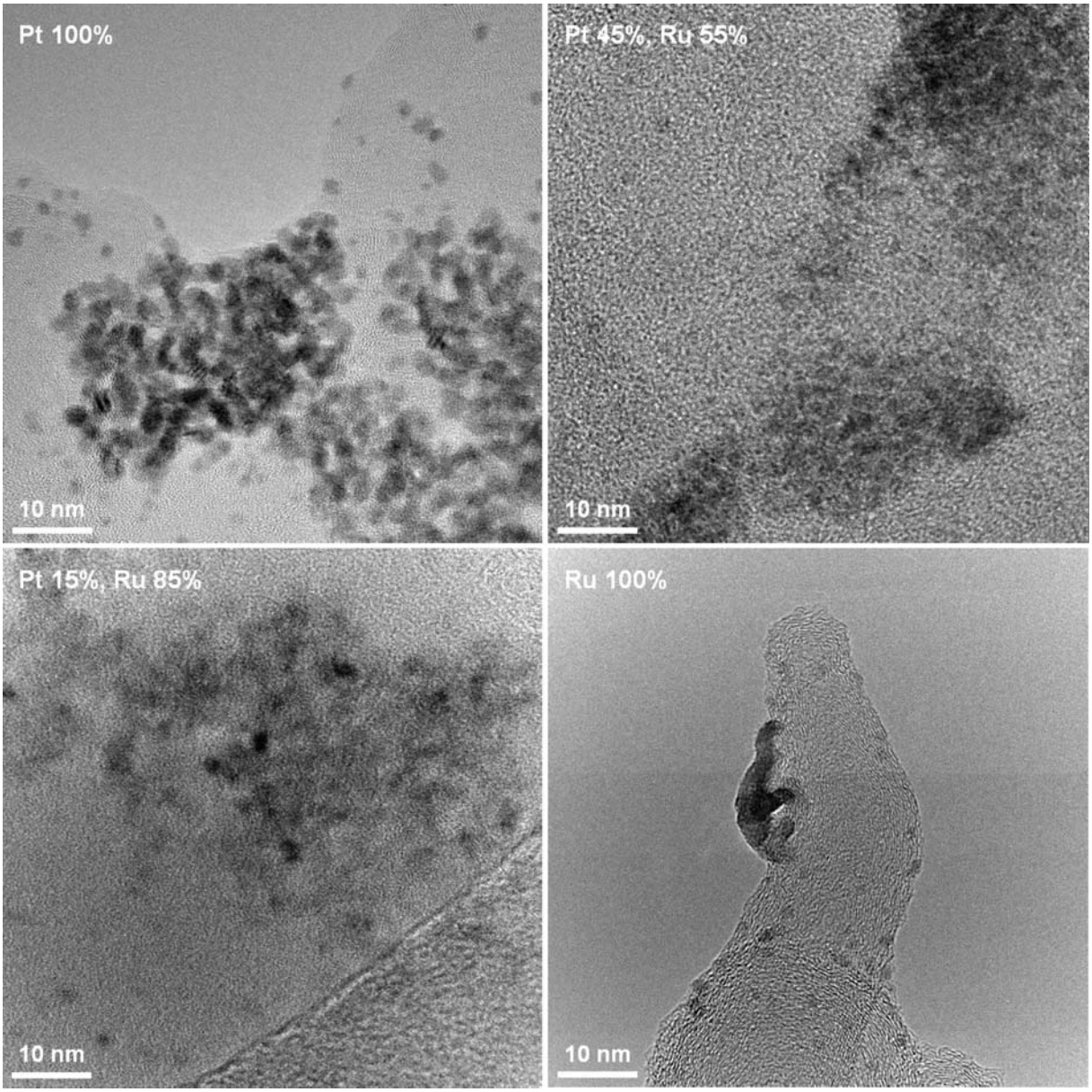

Figure 4. TEM images of different colloid particles on carbon mesh, top left shows pure Pt colloid nanoparticles, top right shows Pt 45%, Ru 55% colloid nanoparticles, bottom left shows Pt 15%, Ru 85% colloid nanoparticles and bottom right shows pure Ru colloid nanoparticles.

the temperature and rate coefficient is plotted versus time. The deactivation of the catalyst is severe, but a constant signal level is approached by the end of the high temperature period. The large change in activity shown is most likely caused by agglomeration and sintering of the colloid nanoparticles into larger particles. This reduces the number of available active surface sites and causes a decrease of the rate constant. This behavior is similar for all investigated colloid compositions. To compare results from different compositions and different reactors all activation cycles and activity measurements are performed identically.

In figure 7, data from an activity measurement obtained in the same reactor is shown. At the highest temperature (340 °C) a slight deactivation is still seen. The change in rate constant with temperature is approximately exponential as predicted from the Arrhenius equation.

To find the apparent activation energy, the activity data for both the up and down ramping of temperature are displayed in an Arrhenius plot for a temperature interval from 282 to 333 °C. In figure 8, activity data for three of the six investigated colloid compositions, and for pure Pt, are shown. The Arrhenius plots show good linearity over the chosen temperature range, but a decreased signal to noise ratio at low conversions is clearly observed in the data for Pt 100% and Pt 30%, Ru 70%. The data for pure Ru colloid particles (not

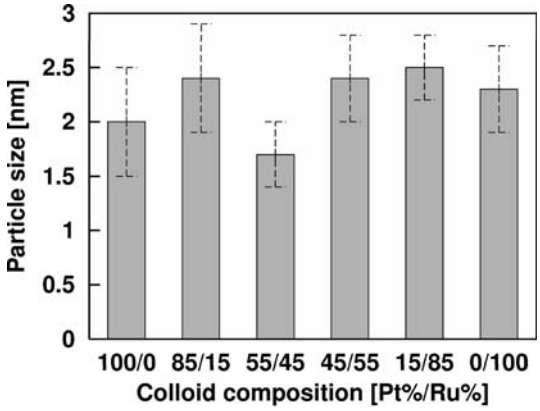

Figure 5. Size distributions from TEM of colloid nanoparticles with different compositions. The error bars indicate the standard deviation on the nanoparticle size.

Table 1
Metal composition of colloids and colloidal solution

Mole %	Pt 10^{-3} M	Ru 10^{-3} M	$E_{app.}$ kJ/mol
Pt 100%	8.2	0	52
Pt 85%, Ru 15%	6.8	1.2	65
Pt 55%, Ru 45%	4.5	3.7	117
Pt 45%, Ru 55%	3.6	4.5	105
Pt 30%, Ru 70%	2.6	6.2	49
Ru 100%	0	8.2	21

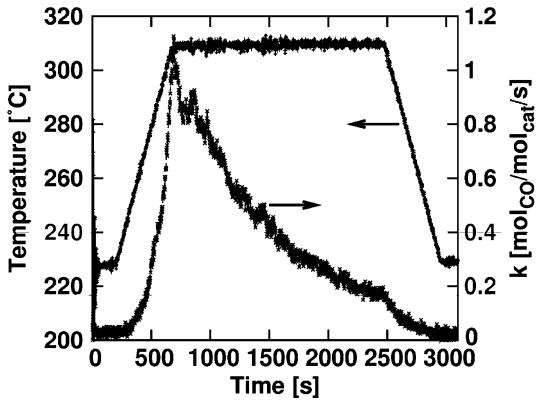

Figure 6. Catalytic activation of Pt 55%, Ru 45% colloid in a gas flow of 1 mL/min. The temperature and rate coefficient is plotted as function of time.

shown) are quite uncertain due to the very low conversion (< 1%). The apparent activation energies for all the different compositions are collected in table 1.

In literature, the activation energy for platinum is found to be 40–60 kJ/mol on a support with low surface area [24, 25], which fits well with the results obtained here. For ruthenium the activation energy found in literature is 48 kJ/mol on Al_2O_3 [26]. It has not been possible to find comparable data for the activation energies for alloys of PtRu.

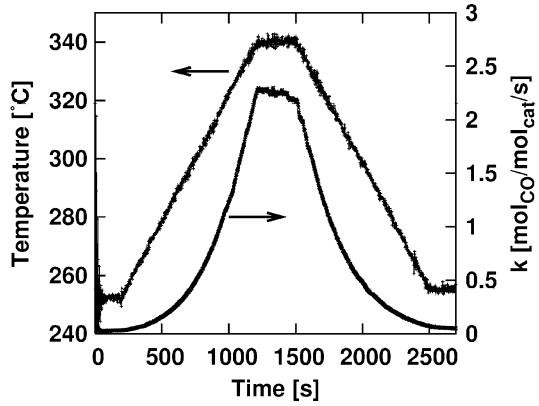

Figure 7. Catalytic activity for Pt 55%, Ru 45% colloid in a gas flow of 0.5 mL/min. The temperature and rate coefficient is plotted as function of time.

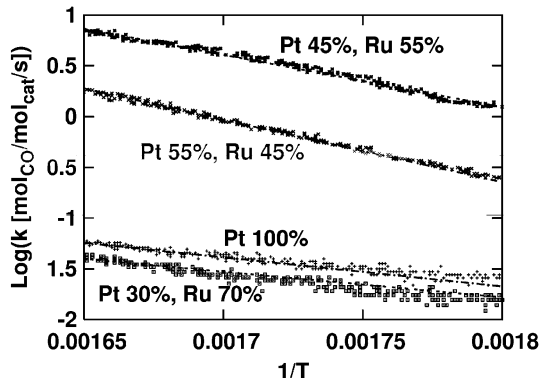

Figure 8. Arrhenius plots for four different colloid nanoparticles Pt 45%, Ru 55%; Pt 55%, Ru 45%; Pt 100% and Pt 30%, Ru 70% in the interval from 555 K to 606 K.

Figure 9 shows that alloying Pt and Ru in colloid nanoparticles gives catalysts with increased activity, and that the composition of 45% platinum and 55% ruthenium gives an activity that is two orders of magnitude higher than the pure metals. It is striking that the highest apparent activation energies are found for the

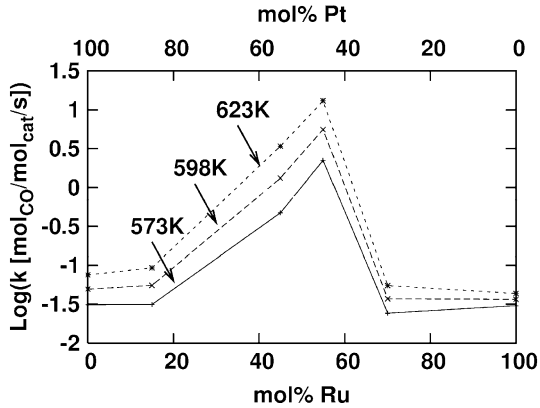

Figure 9. Activity as a function of temperature and composition of the colloid.

compositions with highest activity, which shows that lowering the activation energy does not always increase the reaction rate.

On the pure surfaces the desorption energies for CO on Pt (134 kJ/mol) and Ru (160 kJ/mol) [27] cause the surfaces to be almost fully covered by CO leaving few sites for oxygen. This limits the reaction rate. Calculations on an alloyed Pt/Ru (50%/50%) surface show a significantly reduced desorption energy in the range of 70 kJ/mol [13]. At the temperatures relevant for the present study this leaves plenty of free sites for oxygen to adsorb. This could explain the increased activity of the alloyed colloids close to the 50%/50% Pt/Ru ratio. Of course the calculations are based on a single crystal surface with equal amounts of Pt and Ru in the surface. It is not clear how these results apply to small particles. Furthermore, only the average compositions of the colloid particles are known and the surface composition of the particles might deviate significantly due to the different surface energies of Pt and Ru and due to adsorbate induced segregation [11]. To address these questions is, however, beyond the scope of this study.

4. Conclusion

Microfabricated reactors are shown to be a valuable tool for investigating extremely small amounts of non-porous catalyst.

Alloyed colloid nanoparticles are prepared with different compositions of platinum and ruthenium, and it is found that their sizes are about 2.2 nm independent of composition. This is in accordance with findings from previous studies for non-alloyed colloids.

The catalytic activity was found to describe a volcano curve as a function of the molar composition with a maximum at 45% platinum and 55% ruthenium two orders of magnitude higher than for the pure metals.

Acknowledgments

We thank Jakob Svagin and Flemming Grumsen for experimental assistance. CSG and CINF are sponsored by The Danish National Research Foundation.

References

[1] C. Song, Catal. Today 77 (2002) 17.
[2] J. Larminie, A. Dicks, *Fuel Cell Systems Explained* (Wiley, 2003).
[3] Y. Teng, H. Sakurai, A. Ueda and T. Kobayashi, Int. J. Hydrogen Energy 24 (1999) 355.
[4] G. Avgouropoulos, T. Ioannides and H. Matralis, Appl. Catal. B Environ. 56 (2005) 87.
[5] I.H. Son, A.M. Lane and D.T. Johnson, J. Power Sour. 124 (2003) 415.
[6] Y.-F. Han, M.J. Kahlich, M. Kinne and R.J. Behm, Appl. Catal. B Environ. 50 (2004) 209.
[7] Y.-F. Han, M.J. Kahlich, M. Kinne and R.J. Behm, Phys. Chem. Chem. Phys. 4 (2002) 389.
[8] N. Pavlenko, J.W. Evans, D.-J. Liu and R. Imbihl, Phys. Rev. E. 65 (2001) 016121.
[9] W.-H. Cheng, K.-C. Wu, M.-Y. Lo and C.-H. Lee, Catal. Today 97 (2004) 145.
[10] B.L.M. Hendriksen and J.W.M. Frenken, Phys. Rev. Lett. 89 (2002) 046101.
[11] E. Christoffersen, P. Liu, A. Ruban, H.L. Skriver and J.K. Nørskov, J. Catal. 199 (2001) 123.
[12] J.C. Davies, R.M. Nielsen, L.B. Thomsen, I. Chorkendorff, Á. Logadóttir, Z. Lodziana, J.K. Nørskov, W.X. Li, B. Hammer, S.R. Longwitz, J. Schnadt, E.K. Vestergaard, R.T. Vang and F. Besenbacher, Fuel Cells 4 (2004) 309.
[13] J.C. Davies, J. Bonde, Á. Logadóttir, J.K. Nørskov and I. Chorkendorff, Fuel Cells 5 (2005) 429.
[14] C. Bock, C. Paquet, M. Couillard, G.A. Botton and B.R. Macdougall, J. Am. Chem. Soc. 126 (2004) 8028.
[15] Y. Wang, J. Zhang, X. Wang, J. Ren, B. Zuo and Y. Tang, Top. Catal. 35 (2005) 35.
[16] I. Capek, Adv. Colloid Interface Sci. 110 (2004) 49.
[17] A. Roucoux, J. Schulz and H. Patin, Chem. Rev. 102 (2002) 3757.
[18] U.A. Paulus, U. Endruschat, G.J. Feldmeyer, T.J. Schmidt, H. Bönnemann and R.J. Behn, J. Catal. 195 (2000) 383.
[19] P. Sivakumar, R. Ishak and V. Tricoli, Elektrochim. Acta 50 (2005) 3312.
[20] O. Younes-Metzler, J. Svagin, S. Jensen, C.H. Christensen, O. Hansen and U. Quaade, Appl. Catal. A Gen. 284 (2005) 5.
[21] R.Z. Sørensen, L.J.E. Nielsen, S. Jensen, O. Hansen, T. Johannesen, U. Quaade and C.H. Christensen, Catal. Commun. 6 (2005) 229.
[22] U.J. Quaade, S. Jensen and O. Hansen, Rev. Sci. Instr. 75 (2004) 3345.
[23] U.J. Quaade, S. Jensen and O. Hansen, J. App. Phys. 97 (2005) 44906.
[24] L.S. Sun, S.Y. Li and B.L. Li, React. Kinet. Catal. Lett. 62 (1997) 151.
[25] V.P. Zhdanov and B. Kasemo, Appl. Surf. Sci. 74 (1994) 147.
[26] Y.-F. Han, M. Kinne and R.J. Behm, Appl. Catal. B 52 (2004) 123.
[27] I. Chorkendorff, and J.W. Niemantsverdriet, *Concepts of Modern Catalysis and Kinetics* (Wiley-VCH, 2003).